Proceedings of the 10th International Conference on Structural Health Monitoring of Intelligent Infrastructure, SHMII 10
Porto, Portugal, 30 June - 2 July 2021
A. Cunha, E. Caetano (eds.)

Digital Twin-like Model Updating of a Laboratory Offshore Wind Turbine with Few-Parameters Soil-Structure Interaction Model

A. Abdullahi [1], Y. Wang [1,2]
[1]Department of Civil and Environnemental Engineering, University of Surrey, Guildford, Surrey, GU2 7XH, UK
[2]School of Civil and Environnemental Engineering, Harbin Institute of Technology (Shenzhen), Shenzhen 518055, P. R. China
email : ying.wang@surrey.ac.uk; yingwang@hit.edu.cn

ABSTRACT: Being structures that are highly sensitive to dynamic loads, Offshore Wind Turbines (OWTs) are designed to preclude any sort of resonance. However, during operation, OWTs have been known to experience modal property changes, especially, fundamental natural frequencies, which, once close to the forcing frequencies, can lead to resonance. To avoid this, these structures need to be constantly monitored to assess these modal property changes before they lead to failure. In this study, a digital twin-like model updating is carried out on a laboratory OWT (LOWT) to detect the change(s) in its soil stiffness, occasioned by the application of cyclic loads. To reduce the number of updating parameters, a few-parameters soil-structure interaction (SSI) model is incorporated into the finite element (FE) model of the LOWT, which is created in the commercial software, ANSYS. Two sets of sensing data which are acquired from the prototype LOWT are used for the model updating of the FE model in two respective stages: first, calibration in the original state; and second, update after the application of cyclic loading. For the two updates, the FE model mirrored the conditions of the prototype, based on the modal properties comparison from both, thereby, enabling successful monitoring of the soil stiffness conditions of the LOWT. The results show that soil stiffness increase with the increase in the application of cyclic loading and that the few-parameters SSI model has a high sensitivity to soil stiffness changes. The proposed methodology holds great potential as a model updating system, which draws closer to achieving the digital twin (DT) technology deployment in the monitoring of OWT foundations, and demonstrates the usefulness of a reduced-order SSI model for OWT model updating.

KEYWORDS: Vibration; Offshore wind turbines; Resonance; Digital twin; Model updating; Soil-structure interaction.

1 INTRODUCTION

Offshore wind turbines (OWTs) have recently become very popular as modern societies strive to achieve their future targets of sustainable and environmentally friendly energy utilization. Europe currently leads this charge, with an ambitious target of achieving a 66,488 MW offshore wind turbine capacity to produce 245 TWh of electrical energy by the year 2030 (Corbetta, et al., 2015).

Being a relatively new technology, OWTs have insufficient track records to describe their expected behaviours. This makes them susceptible to possible dangers of unanticipated breakdowns, often requiring unplanned 'costly' maintenance, accompanied by unnecessary downtime(s).

OWTs are highly dynamic structures that must avoid resonance, following which, DNV (2014) recommends that the target fundamental frequency of operating OWT must fit into a narrow band of within 10% more and 10% less of the OWT's 1P and 3P frequencies, respectively, in a design method known as soft-stiff (Lombardi et al., 2013). This thus limits the allowable safe margin of natural frequency change-an inevitable phenomenon with operating OWTs. Where the fundamental frequencies of the OWTs approach those of 1P and 3P, resonance can occur, as has been reported in the tower of the Areva Multi-brid M5000 OWT prototype by Hu et al., (2014). Under the actions of wind, wave, 1P, and 3P, OWTs experience constant vibrations. This leads to the fact that dynamic foundation fixity conditions may change, resulting in the change of modal properties (Bhattacharya et al., 2011; Guo et al., 2015; Xu et al., 2019). Although known to be imminent in operational OWTs, these factors and resulting conditions may ab-initio, be difficult to be accurately predicted due to their strong dependence on nature. To guarantee the safety of operational OWTs, monitoring systems that keep track of the health states of these structures are required at regular time intervals, or better still, in real-time.

As has been widely adopted in various engineering professions, finite element (FE) analysis is heavily employed for the design and evaluation of civil engineering infrastructure. However, most often a time, there exist discrepancies between the FE models and the prototypes they are modelled after, due to damage and/or (over)simplified assumptions of structural geometry, materials, and boundary conditions (Wang and Zhang, 2013). To minimize these discrepancies (for purposes of calibration or damage detection), FE model updating has often been employed (Wang and Zhang, 2013; Xu et al., 2019). The required details for the development of sufficiently accurate FE models for model updating often prove excessive to the allowance of certain model updating algorithms due to the high number of updating parameters involved, inevitably, decreasing the efficiency and processing time of the updating program.

Since modal property changes in operational OWTs are more attributable to soil stiffness alterations, rather than the occurrence of local tower damage (Xu et al., (2019); Lombardi et al., (2013) and Ahmed and Hawlader (2016)), the soil stiffness is considered as an important updating parameter in the monitoring of OWTs. To reduce the number of updating parameters to enhance the updating efficiency, Abdullahi et al., (2020) proposed a few-parameters SSI model for the model updating of Monopile and Jacket supported OWTs, but have not applied the model to the updating process.

Digital Twins (DTs) have increasingly attracted attention around the world due to their ability to link physical assets to their virtual models across different fields, thereby, enabling the emergence of smart infrastructures. Kahlen et al., (2016) regards a digital informational construct about a physical system created as an entity existing on its own as the DT of the latter. Thus, once traditional FE models of physical prototypes can continuously be updated based on acquired real-time sensing data, then they become the virtual representations of the physical assets, and their DTs (Macdonald et al., 2017). Hence, the adoption of a DT-like model updating as the SHM technique of choice for this monitoring task, given its penchant for probing (even) inaccessible parts of infrastructure (buried soil layers).

In this paper, an FE model of an LOWT with few parameters SSI is developed and validated. It allows the direct use of the soil stiffness, rather than the maximum lateral soil resistance and maximum displacement, which is similar, but slightly advanced to that proposed by Abdullahi et al., (2020). Then, an experimental modal test on the prototype LOWT is performed to obtain its sensing data. Finally, the concept of DT through a two-stage updating of the FE model is implemented on the LOWT model. The updated FE model is studied to reveal the soil stiffness change in the prototype after undergoing the cyclic load application.

2 METHODOLOGY

2.1 Numerical model of LOWT

The prototype used in Xu et al., (2019) is adopted in this study due to its relevance. This is made up of an assembly of a hollow monopile, transition piece, hollow tower, and a lumped mass (representing the rotor-nacelle assembly). The monopile is inserted to a depth, d, of 328 mm, into the red-hill silica sand medium contained in a rectangular sand box-made of plastic. The tower and monopile are made of aluminium alloy, both having an external diameter of 41 mm, and a thickness of 0.75 mm, while their lengths are 1000 and 350 mm, respectively. The transition piece is 694 g, and with the aid of bolts, fastens the tower to the monopile, which is also made of aluminium alloy. The lumped mass is an 824 g rectangular aluminium alloy sitting on top of the tower. Finally, the prototype is instrumented with two 140 g accelerometers located at 1000 mm (L) and 700 (0.7L) from the mudline. Figure 1 shows a schematic diagram of the described LOWT set-up.

2.2 Finite element (FE) model of LOWT

Based on the simple geometry of the prototype, a 2-D FE model of the LOWT is developed in the commercial software, ANSYS v19.1, as shown in Figure 2. The tower and monopile are modelled by a beam element (BEAM188 in ANSYS) as this conveniently accommodates the lumped masses, as well as the soil springs. A roller boundary condition is specified at the end-bearing part of the monopile (Carswell et al., 2015). The top, accelerometer, and the transition piece masses, are modelled by a mass element (MASS21 in ANSYS). The interaction between the buried length of the monopile and the soil (SSI) is simulated by nonlinear Winkler soil springs (COMBIN39 in ANSYS), based on API (2010).

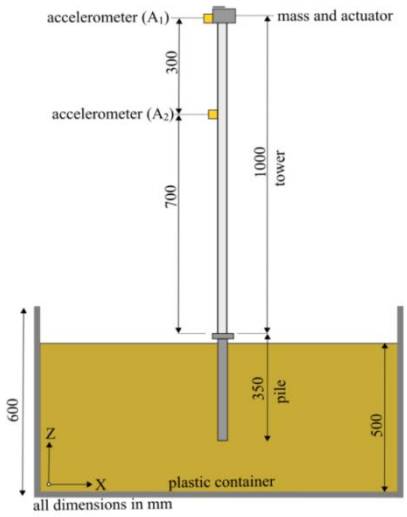

Figure 1. Schematic diagram of the LOWT set-up.

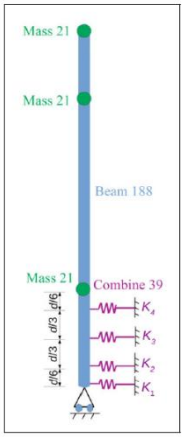

Figure 2. FE model of LOWT (Xu et al., 2019)

2.3 Soil structure interaction (SSI)

Soil-structure interactions significantly impact the modal properties of OWTs. According to Jalbi et al., (2017), SSI simulation methods can broadly be grouped into three: simplified, standard and advanced methods. The distributed nonlinear spring model (*p-y*, *t-y* and *Q-p*) used in del Campo et al., (2015); Harte & Basu, (2012) constitutes the standard method; the simplified methods include both the three-springs model (lateral, rotational and vertical springs, described in Schafhirt et al. (2016)) and four-spring models (lateral, rotational, vertical and rotational-lateral coupled springs, as described in Lombardi et al. (2013) and Arany et al. (2017)). The advanced method involves the use of FE analysis along with sophisticated soil models, e.g. Huang et al. (2009).

To achieve a good balance between FE modelling accuracy and ease of implementation, the standard SSI method is adopted in this study. Since the lateral loads on OWTs from wind and waves far outweigh those from their self-weights, load capacities in the lateral direction play the most significant role in stabilizing their foundations (Abdullahi et al., 2020). As recommended in API (2010), discrete *p-y* springs account for lateral soil stiffness against foundation movement, and the spacing between successive sets on a pile, are chosen based on the aim of the study. For example, Bisoi and Haldar (2014)

modelled the springs with 1m spacing, while Zuo et al. (2018) chose 10 m spacing. In this study, the spacing is selected as 54.7mm between the mudline and top-spring, as well as between bottom spring and third, while a spacing of 109.3 mm is chosen between the other springs (Xu et al., 2019).

Dense sand is used as the support medium housing the LOWT foundation. As per API (2010), the lateral soil resistance per unit length of the pile, p, (N/m) is related to its unit deflection, y, by the expression:

$$p = A \cdot pl \cdot \frac{\tanh(k.H)}{A \cdot pl} \cdot y \quad (1)$$

where A is a factor accounting for cyclic or static loading conditions:

$$A = 0.9 \text{ for cyclic loading} \quad (2)$$

$$A = (3.0 - 0.8\frac{H}{D}) \geq 0.9 \text{ for static loading} \quad (3)$$

k is the initial modulus of subgrade reaction (kN/m^3); y is the lateral deflection (m), and D is the average pile diameter (m). pl is the ultimate unit lateral bearing capacity of the soil (N/m) at depth H (m), which varies from shallow (pls) to deep depths (pld). They can be estimated based on the following formulations (API 2010):

$$pls = (C_1.H + C_2.D)\gamma.H \quad (4)$$

$$pld = C_3.D.\gamma.H \quad (5)$$

$$pl = \min(pls, pld) \quad (6)$$

where γ is the effective soil weight (kN/m^3); C_1, C_2 and C_3 are coefficients determined as functions of the angle of internal friction, ϕ (degrees).

In this study, C_1, C_2, C_3 and k are determined for Red Hill Silica sand with basic properties as follows:

$\gamma = 16.8kN/m^3, \phi = 36^\circ$ (Abdullahi et al. 2020).

Based on the formulation above, the p-y curves simulating the SSI of the LOWT model are obtained and used for the development of the few parameters SSI used for the updating program.

2.4 *Few-parameters SSI*

The soil p-y curves in Xu *et* al., (2019) are utilized in the development of the few-parameters SSI model of the LOWT. The maximum lateral resistance, p_{max}, of the soil supporting the LOWT superstructure, is chosen as the target parameter influencing the soil stiffness, and by extension, the natural frequency of the entire systems. For each considered depth, *H (m)*, along the pile lengths, p_{max} *(N)* occurring at the point of maximum lateral displacement, y_{max} *(m)*, is obtained; Relying on the fact that the p-y soil springs for the LOWT foundation exhibit elastic-plastic deformations, the formulation for estimating soil stiffness, K (N/m), described in Augustesen, et al. (2009), is utilized. For any considered depth *H (m)*, along the pile length, the p_{max}, along with its corresponding y_{max} values from the p-y curve, are used to compute the soil stiffness as given in Equation (7).

$$K_j = (p_{max\,j})/(y_{max\,j}) \quad (7)$$

These stiffness values from the p-y curve are 2.7 x 10^5, 2.6 x 10^5, 2.1 x 10^5, 8.8 x 10^4 N/m, for the four considered soil layers $(d, 5d/6, d/2, d/6)$ from the bottom, respectively. A plot of K against H values along the pile length is then made, wherefrom, a curve describing the relationship between the two parameters emerges, onto which a polynomial equation is fitted. Since we assume that there is no displacement at the interface between mudline and the exposed pile, (K = 0 when H = 0), the constant term is therefore set as 0.

$$K = \sum_{i=1}^{n} \propto_i H^i \quad (8)$$

where $\propto_i$ represents constants (in this case, defined by soil properties and foundation form/geometry), while n is the degree of the polynomial equation defining K and H relationship. This single equation defines K for any depth along the length of the buried pile, thereby reducing an otherwise elaborate model to a few-parameters one.

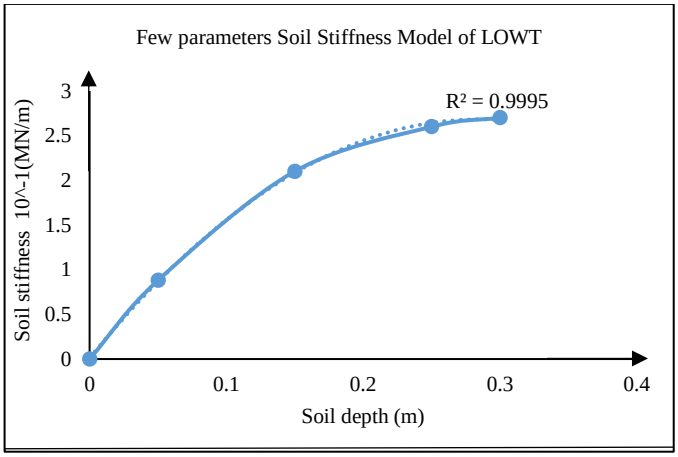

$$K = -32.898 \times 10^5 \times H^2 + 18.746 \times 10^5 \times H \quad (10)$$

Figure 3. Plot of initial soil stiffness against depth for the LOWT.

2.5 *Model updating*

In this study, sensing data from the LOWT are obtained in the first stage. In the second stage, the sensing data are processed to obtain damage sensitive parameters, in this case, natural frequencies and mode shapes (using ARTEMIS software). In the third stage, the damage sensitive parameters are used to iteratively update the FE model until the damage sensitive parameters from the updated FE model match the processed sensing data.

The FE model updating is conducted on the reduced-order FE model (made up *2.2* and *2.4*) based on Estimation of Distribution Algorithms (EDAs). The algorithm involves the selection of individuals based on the prescribed objective function, learning and sampling to generate new individuals for the next generation, and finally, replacing ineffective individuals. EDA permits numerous implementation strategies including the incorporation of new methods by users, while the Mateda-2.0 is still regarded as the most practical (Santana et al., 2010) of these strategies.

Due to its ease of implementation and proven efficiency in solving similar problems, the Gaussian network model is adopted for use here. The stiffness of the pile-surrounding soil is chosen as the updating parameter. Two of the objective

functions proposed by Wang and Zhang (2013) are chosen for the EDA implementation as shown in Equations (11) and (12).

$$J_1 = \sum_{i=1}^{m}(f_{ai} - \frac{f_{ei}}{f_{ei}})^2 \quad (11)$$

$$J_2 = \sum_{j=1}^{m}\sum_{j=1}^{m}\cdot(\frac{\phi_{ai}\cdot\phi_{ajT}}{f_{ai}^2} - \frac{\phi_{ei}\cdot\phi_{Tej}}{f_{ai}^2})^2 \quad (12)$$

where f_i represents the i th natural frequency; ϕ_i and ϕ_j represent the ith and jth mode shapes, respectively, while a and e respectively represent the analytical and experimental (true) results. From figure 4, the model updating process is completed at the convergence of either J_1 or J_2 to zero, or after the specified number of generations is reached.

The soil stiffness at any given depth along the pile length is specified by Equation (10), with two updating parameters: $\propto_1 = -32.898E5$ and $\propto_2 = 18.746E5$, which are used for the model updating operation instead of four (for standard method). The plot captures the stiffness-depth relationship to a sufficient accuracy with an R^2 value of almost 1, at 0.9995, indicating a good match.

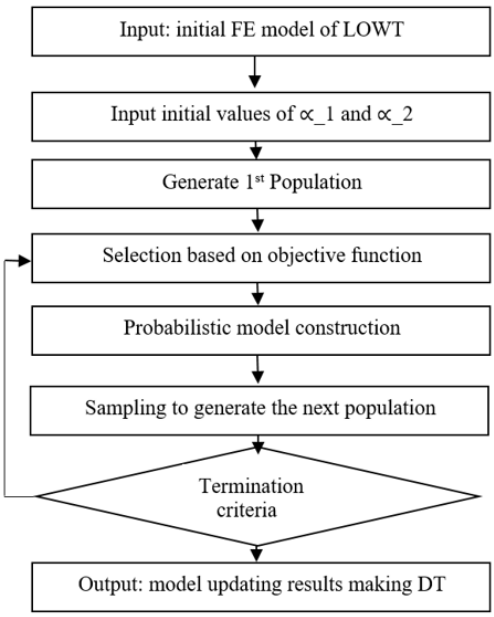

Figure 4. Flowchart of EDA based DT formation

3 EXPERIMENTAL STUDIES

3.1 Modal test description

The modal tests were conducted in the Surrey Advanced Geotechnical Engineering (SAGE) laboratory at the University of Surrey, UK, building on previous research in the same laboratory (Xu et al., 2019). Following the instrumentation of the LOWT model, three different tests involving free vibration and cyclic loading tests were conducted. For the free vibration tests, a 4.45 kN impact hammer was used to generate impact loads and vibration signals (acceleration) which were recorded by a standard sensing system (National Instrument compact data acquisition module, cDAQ-9174). The cyclic loading test involved the use of an excitation apparatus similar to that described in Nikitas et al., (2016) to deliver load cycles to the LOWT. To obtain the calibration inputs for the FE model, a free vibration test was conducted on the prototype to obtain acceleration signals, which were processed to obtain the first natural frequency as well as its accompanying mode shapes at L and 0.7L. Second, an excitation apparatus similar to that described in Nikitas et al., (2016) was used to deliver an 8.8 x 10^5load cycles at a force of 1 N per cycle, to the top of the prototype. This caused a continuous vibration of the prototype in a manner that mimicked the vibration of an operational OWT throughout the loading process. In the third test following the cyclic load application, another free vibration test was conducted to obtain a new first natural frequency and its accompanying mode shapes at the same positions as above.

3.2 Results

Following the initial free vibration test, acceleration signals were recorded by the sensing system. Using the highly accurate modal analysis software, ARTEMIS modal v6.1, the various acceleration time histories were obtained and processed into frequency signals to obtain the first natural frequency of the LOWT as well as their mode shapes, typical examples of which are shown in Figures 5 a and b. To obtain the first update inputs (i.e., second set of modal properties), a similar operation to the one described above was conducted. Table 1 shows the obtained modal properties of the LOWT throughout the two free vibration tests.

Table 1. Experimental Modal Results of LOWT

	Calibration Modal test	Modal test after Cyclic loading
Natural frequency (Hz)	6.541	6.872
Mode shape at L	0.8583	0.8650
Mode shape at 0.7L	0.5600	0.5020

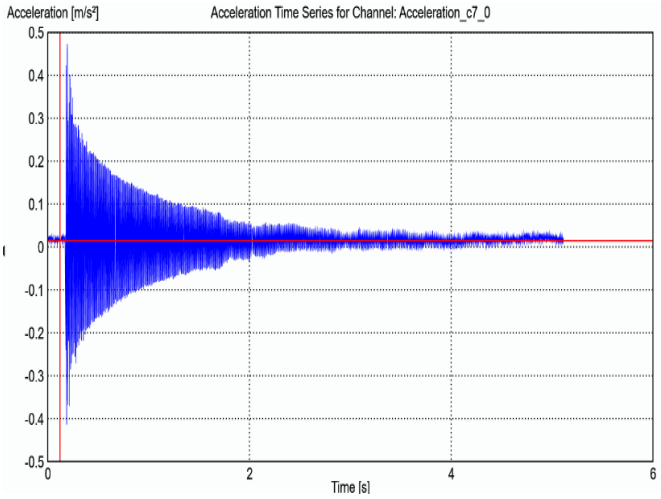

Figure 5 a. Typical acceleration time history from a free vibration test on the LOWT in ARTEMIS.

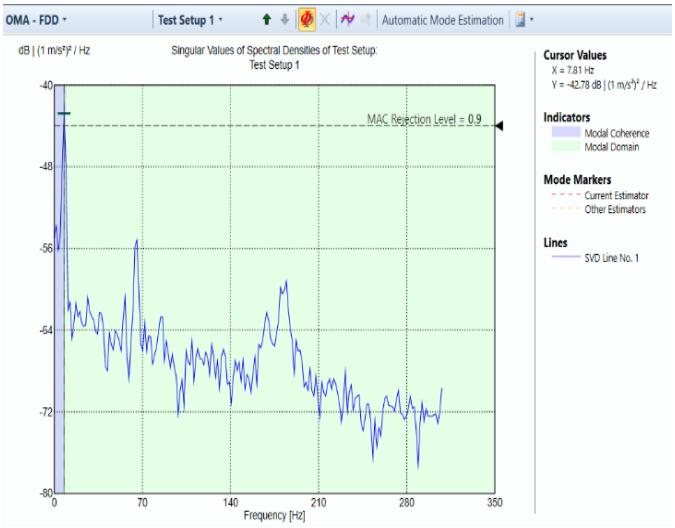

Figure 5 b. Typical Modal analysis result showing the natural frequency of the LOWT in ARTEMIS.

4 MODEL UPDATING

4.1 Model updating results

In the first instance, the model updating program is applied to the LOWT FEM in a calibration operation. The first natural frequency and its corresponding mode shapes at L and 0.7L are obtained and compared to the experimental results from the first free vibration test. Very close agreements are observed, thereby signalling the successful calibration of the initial FE model and setting the stage for the creation of the LOWT digital twin. In the second stage, the results of the free vibration test (modal properties) following the cyclic load application are used to update the initially calibrated FE model. Again, very close agreements between the considered natural frequencies and their corresponding mode shapes are observed. It has been shown across the two sets of model updating conducted, through the results obtained, that the FE model was continuously updated to reflect the modal properties obtained from the experiments. Figure 6 is similar to Figure 3 and shows the changes in the soil stiffness across the four considered depths from calibration, to the update after cyclic load application. Expanding the stiffness equation at any depth from Figure 8 given by Equations (13) and (14), the soil stiffness at that depth is obtained, and upon comparing the stiffness value after and before a load application, the amount of stiffness change along with the change position is obtained.

For validation, a similar operation as the one above is conducted using the standard SSI soil stiffness model with four updating parameters. Across the updated natural frequencies and mode shapes, the results from the proposed method show very close agreements with the true values and matches very closely, the performance of the standard SSI method of model updating. Average differences of only 0.018 and 2.95 % for natural frequencies and mode shapes are respectively observed compared to the experimental values using the proposed method. The standard method, on the other hand, recorded differences of 0.0 and 2.933 % in similar steads as shown in Tables 2 and 3 as well as pictorial depictions from Figures 7 and 8, respectively. The slight difference in the accuracy of the results between the proposed and standard methods may be due to the R^2 value in the base stiffness equation which forms the basis of formulating the updating parameters (i.e., Equation (10)), which is although very close to 1, falls slightly short. These results lend credence to the use of reduced-order FE model for use in model updating in SSI operations.

Table 4 shows the updated soil stiffness across the considered soil layers from calibration to the update after the application of cyclic loading. Where K' represents the updated stiffness, and K represents the calibrated stiffness. For the calibration cases, K' represent the calibrated stiffness, while K represents the initially estimated soil stiffness. The change in soil stiffness values is observed to be more pronounced with the use of the proposed methodology than standard SSI.

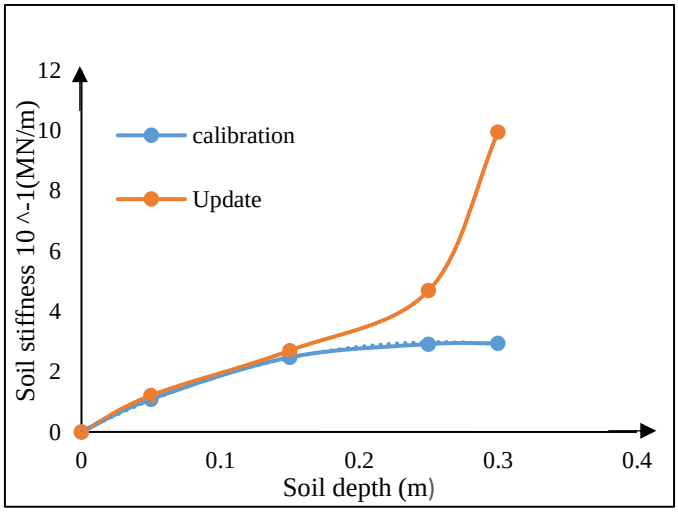

Figure 6. Plot of calibrated/updated soil stiffness against the depth of the LOWT

$$K = -4 \times 10^6 \times H^2 + 2 \times 10^6 \times H \quad (13)$$

$$K = 10^7 \times H^2 - 2514H \quad (14)$$

Equations (13) and (14) are the respective stiffness equations of calibration and update of the LOWT model.

Table 2. Performance of the proposed and standard model updating methods against the true values using natural frequency convergence.

Frequency	True value (Hz)	Proposed SSI (Hz)	Standard SSI (Hz)
Calibration	6.541	6.542	6.541
After cyclic load	6.872	6.871	6.872
Difference (%)		0.018	0.000

Table 3. Performance of proposed and standard model updating methods against true values using mode shape convergence

Mode shape	True value	Proposed SSI	Standard SSI
L: Calibration	0.858	0.861	0.861

L: After cyclic load	0.865	0.843	0.842
0.7L: Calibration	0.560	0.562	0.562
0.7L: After cyclic load	0.502	0.545	0.544
Average difference (%)		2.950	2.933

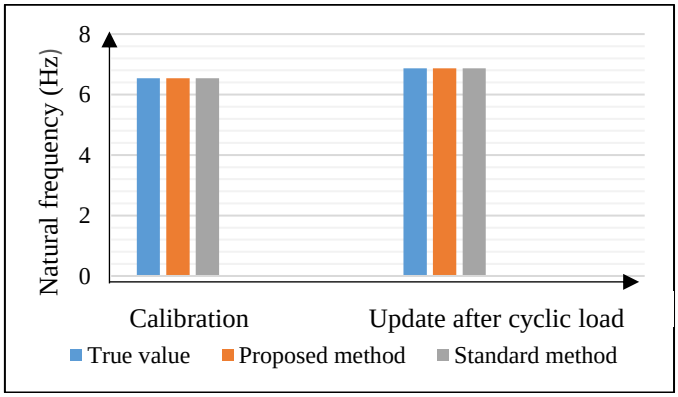

Figure 7. Model Updating performance of the proposed and standard methods against true values using natural frequencies.

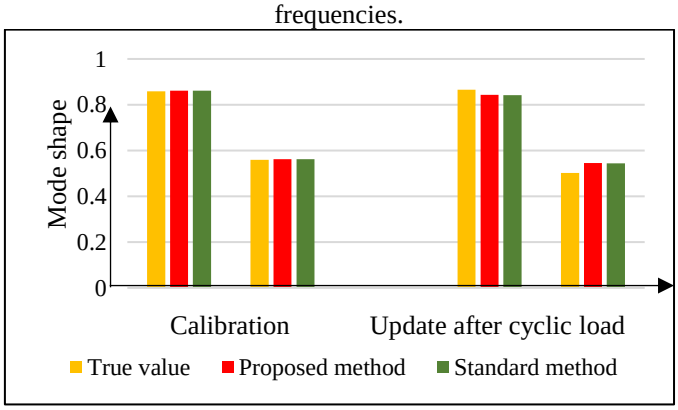

Figure 8. Model Updating performance of the proposed and standard methods against true values using mode shapes

Table 4. Comparison of Updating factors from the proposed and standard SSI methods

		$\frac{K1'}{K1}$	$\frac{K2'}{K2}$	$\frac{K3'}{K3}$	$\frac{K4'}{K4}$
Calibration	Proposed SSI	1.23	1.18	1.12	1.09
Calibration	Standard SSI	1.21	1.14	1.09	1.07
Update	Proposed SSI	1.12	1.09	1.61	3.38
Update	Standard SSI	1.08	1.03	1.446	3.104

4.2 Discussion of results

Based on the results, the updating performance of the proposed methodology possesses a lot of promise, especially as it matched the standard SSI method as well as the experimental results with both natural frequency and mode shapes very closely. As shown in Tables 2 and 3, the proposed methodology recorded 99.98 and 97.05 % agreements with the true values in natural frequencies and mode shapes, respectively, while recording agreements of over 99 % in both natural frequencies and mode shapes with the standard method results.

In terms of sensitivity to soil stiffness changes, the proposed methodology tends to be more sensitive than the standard method. This is evident in the observed slightly higher soil stiffness change rates recorded across all the considered soil layers after the updating process, as shown in Table 4. This advantage makes the proposed method a valuable tool for deployment in DT technology for soil stiffness monitoring of OWTs because such high sensitivity will very well suit real-time monitoring through an ability to pick up slight and temporal soil stiffness changes. Also, this method possesses the additional advantage of predicting the soil stiffness of points whose initial values are not known along the pile. Although the stiffness change after the cyclic load application varies somewhat from the standard SSI results, the trend in both cases was generally aligned. It is also observed from the updated stiffness results using both methods that the top half layers of the soil are more sensitive than the bottom. This is expected as the latter is closest to the end bearing part of the pile where the degree of freedom is highly negligible, thereby experiencing more restraints in movement during the vibration. This constrained vibration effect leads to little or no densification/compaction of the soil, resulting in largely unchanged soil stiffness conditions. It is important to note that the observed behavior here is in agreement to findings from a similar research by Xu et al., (2019). Further development of this methodology will be explored in future studies.

5 CONCLUSIONS

In this paper, a reduced-order finite element model updating methodology is applied to soil stiffness monitoring of OWTs using model updating. Use is made of the EDA model updating program with two updating parameters instead of four (for standard SSI method). This achieves highly accurate results over a two-stage DT-like updating of the FE model. Natural frequencies and mode shapes obtained at each stage of the experimental modal testing conducted on the LOWT are used as the true values throughout the study. With each successful update, the LOWT FE model becomes a virtual model of the physical LOWT, hence its DT. This DT is used to gain an insight into the soil stiffness condition (change) of the LOWT model at any point after the cyclic load application. Soil stiffness is found to increase substantially with increase in cyclic loading in the top half of the soil, while experiencing negligible changes in the bottom half. From the top, the first layer experienced an increase of stiffness amounting to about 210%, while the second experienced an increase of about 45%. The third and fourth layers experienced stiffness changes below 10%.

The proposed SSI methodology is found to be more sensitive to soil stiffness change than the standard SSI method, and in terms of convergence, the former performed very closely accurately to the latter in both natural frequency and mode shape comparisons.

With such easily implementable few-parameters SSI model updating methodology, along with fast modal analysis software, such as ARTEMIS, DT realization in its optimum form for soil stiffness monitoring, can soon become a popular reality.

ACKNOWLEDGEMENT

The first author would like to acknowledge the support of Petroleum Technology Development Fund (PTDF) under the Federal government of Nigeria, for sponsoring his PhD studies.

REFERENCE:

1. Corbetta, G., Ho, A., Pineda, I., Ruby, K., 2015. Wind energy scenarios for 2030. *Ewea*, (July), pp. 1–8. Available at: http://www.ewea.org/fileadmin/files/library/publications/reports/EWEA-Wind-energy-scenarios-2030.pdf
2. Bhattacharya, S., Lombardi, D. and Muir Wood, D., 2011. Similitude relationships for physical modelling of monopile-supported offshore wind turbines. *International Journal of Physical Modelling in Geotechnics*, *11*(2), pp.58-68.
3. Guo, Z., Yu, L., Wang, L., Bhattacharya, S., Nikitas, G. and Xing, Y., 2015. Model tests on the long-term dynamic performance of offshore wind turbines founded on monopiles in sand. *Journal of Offshore Mechanics and Arctic Engineering*, *137*(4).
4. Xu, Y., Nikitas, G., Zhang, T., Han, Q., Chryssanthopoulos, M., Bhattacharya, S. and Wang, Y., 2020. Support condition monitoring of offshore wind turbines using model updating techniques. *Structural health monitoring*, *19*(4), pp.1017-1031.
5. DNV, G., 2014. DNV-OS-J101–Design of offshore wind turbine structures. *DNV GL: Oslo, Norway*.
6. Lombardi, D., Bhattacharya, S. and Wood, D.M., 2013. Dynamic soil–structure interaction of monopile supported wind turbines in cohesive soil. *Soil Dynamics and Earthquake Engineering*, *49*, pp.165-180.
7. Hu, W.H., Thöns, S., Said, S. and Rücker, W., 2014. Resonance phenomenon in a wind turbine system under operational conditions. *structural health monitoring*, *12*, p.14.
8. Kahlen, F.J., Flumerfelt, S. and Alves, A., 2017. Transdisciplinary Perspectives on Complex Systems. *Transdisciplinary Perspectives on Complex Systems: New Findings and Approaches*.
9. Macdonald, C., 2017. Creating a Digital Twin for a Pump. *Ansys Advantage Issue*, *1*. *Available at*: http://www.ansys.com//media/Ansys/corporate/resourcelibrary/article/Creating-a-Digital-Twin-for-a-Pump-AA-V11-I1.pdf.
10. Wang, Y. and Zhang, T., 2013, January. Finite element model updating using estimation of distribution algorithm. In *SHMII-6 2013: Proceedings of The 6th International Conference on Structural Health Monitoring of Intelligent Infrastructure* (pp. 1-8). Hong Kong Polytechnic University.
11. Abdullahi, A., Wang, Y. and Bhattacharya, S., 2020. Comparative Modal Analysis of Monopile and Jacket Supported Offshore Wind Turbines including Soil-Structure Interaction. *International Journal of Structural Stability and Dynamics*, *20*(10), p.2042016.
12. Ahmed, S.S. and Hawlader, B., 2016. Numerical analysis of large-diameter monopiles in dense sand supporting offshore wind turbines. *International Journal of Geomechanics*, *16*(5), p.04016018.
13. del Campo, Vanessa, Daniele Ragni, Daniel Micallef, Francisco Javier Diez, and CJ Simão Ferreira. "Estimation of loads on a horizontal axis wind turbine operating in yawed flow conditions." *Wind Energy* 18, no. 11 (2015): 1875-1891.
14. Harte, M., Basu, B. and Nielsen, S.R., 2012. Dynamic analysis of wind turbines including soil-structure interaction. *Engineering Structures*, *45*, pp.509-518.
15. Schafhirt, S., Page, A.M., Eiksund, G.R. and Muskulus, M., 2016. Influence of soil parameters on the fatigue lifetime of offshore wind turbines with monopile support structure.
16. Arany, L., Bhattacharya, S., Macdonald, J. and Hogan, S.J., 2017. Design of monopiles for offshore wind turbines in 10 steps. *Soil Dynamics and Earthquake Engineering*, *92*, pp.126-152.
17. Huang, B., Bathurst, R.J. and Hatami, K., 2009. Numerical study of reinforced soil segmental walls using three different constitutive soil models. *Journal of Geotechnical and Geoenvironmental engineering*, *135*(10), pp.1486-1498.
18. Zwerneman, F. J., & Digre, K. A., 2010. 22nd edition of API RP 2A recommended practice for planning, designing and constructing fixed offshore platforms - Working stress design. *Proceedings of the Annual Offshore Technology Conference*, *3*(December 2000), 2364–2372.
19. Bisoi, S. and Haldar, S., 2014. Dynamic analysis of offshore wind turbine in clay considering soil–monopile–tower interaction. *Soil Dynamics and Earthquake Engineering*, *63*, pp.19-35.
20. Zuo, H., Bi, K. and Hao, H., 2019. Mitigation of tower and out-of-plane blade vibrations of offshore monopile wind turbines by using multiple tuned mass dampers. *Structure and Infrastructure Engineering*, *15*(2), pp.269-284.
21. Nikitas, G., Vimalan, N.J. and Bhattacharya, S., 2016. An innovative cyclic loading device to study long term performance of offshore wind turbines. *Soil Dynamics and Earthquake Engineering*, *82*, pp.154-160.
22. Santana, R., Bielza, C., Larranaga, P., Lozano, J.A., Echegoyen, C., Mendiburu, A., Armananzas, R. and Shakya, S., 2010. Mateda-2.0: Estimation of distribution algorithms in MATLAB. *Journal of Statistical Software*, *35*(7), pp.1-30.